Journal of Energy Chemistry 81 (2023) 313–320

Contents lists available at ScienceDirect

Journal of Energy Chemistry

journal homepage: www.elsevier.com/locate/jechem

http://www.journals.elsevier.com/journal-of-energy-chemistry/

Review

Deep dive into anionic metal-organic frameworks based quasi-solid-state electrolytes

Tingzheng Hou [a,*], Wentao Xu [b,*]

[a] Institute of Materials Research, Tsinghua Shenzhen International Graduate School, Tsinghua University, Shenzhen 518055, Guangdong, China
[b] John A. Paulson School of Engineering and Applied Sciences, Harvard University, Cambridge, MA 02138, USA

ARTICLE INFO

Article history:
Received 17 February 2023
Revised 24 February 2023
Accepted 26 February 2023
Available online 9 March 2023

Keywords:
Anionic metal–organic frameworks
Quasi-solid-state electrolytes
Ionic conduction
Lithium metal batteries
Lithium-ion batteries

ABSTRACT

The development and application of high-capacity energy storage has been crucial to the global transition from fossil fuels to green energy. In this context, metal–organic frameworks (MOFs), with their unique 3D porous structure and tunable chemical functionality, have shown enormous potential as energy storage materials for accommodating or transporting electrochemically active ions. In this perspective, we specifically focus on the current status and prospects of anionic MOF-based quasi-solid-state-electrolytes (anionic MOF-QSSEs) for lithium metal batteries (LMBs). An overview of the definition, design, and properties of anionic MOF-QSSEs is provided, including recent advances in the understanding of their ion transport mechanism. To illustrate the advantages of using anionic MOF-QSSEs as electrolytes for LMBs, a thorough comparison between anionic MOF-QSSEs and other well-studied electrolyte systems is made. With these in-depth understandings, viable techniques for tuning the chemical and topological properties of anionic MOF-QSSEs to increase Li^+ conductivity are discussed. Beyond modulation of the MOFs matrix, we envisage that solvent and solid–electrolyte interphase design as well as emerging fabrication techniques will aid in the design and practical application of anionic MOF-QSSEs.

1. Definition, categorization, and classification

The ever-increasing demand for portable electronic devices, electric vehicles, and smart grids powered by intermittent solar/wind energy has made high-capacity energy storage technology crucial [1–3]. Conventional lithium-ion batteries (LIBs) with a composition of $LiCoO_2$/graphite have been commercialized for more than three decades, yet the underlying intercalation chemistry is approaching the limit of its capability [4]. The revival of lithium metal batteries (LMBs) has therefore become a necessity. Lithium metal anode by definition has the highest theoretical capacity (3,860 mA h g^{-1}, or 2,061 mA h cm^{-3}) and the lowest electrochemical potential (−3.04 V versus the standard hydrogen electrode) among all possible candidates, making it the ultimate choice for the anode in a lithium battery [5,6]. However, uncontrolled lithium decomposition during plating/stripping, typically resulting in dendritic and mossy lithium, can cause cell failure and even thermal runaway, leading to fire/explosion events [7–9]. These safety concerns have largely plagued the practical applications of LMBs. Li dendrites are generally induced by the inhomogeneous distribution of space charge, high current density on the anode surface, and the cracking of the solid electrolyte interphase (SEI) [10]. Considerable effort has been devoted to the development of novel ion-conducting materials to prevent Li dendrite growth in a working battery [11]. While novel electrolyte additives such as FEC can improve cycling performance [12], the potential risks of thermal runaway still remain. To address this challenge, one straightforward and promising approach is to substitute the conventional separator and liquid electrolyte design with high-mechanical-strength and dense solid-state electrolytes (SSEs) [13–16].

Metal–Organic Frameworks (MOFs) with an interconnected pore system and a three-dimensional crystalline structure composed of coordinately linked metal ions/clusters and organic ligands have been utilized as Li^+-conducting solid matrices since 2011 [17–26]. Due to the tunable porosity resulting from the enormous chemical and structural diversity [27], MOFs are ideal materials for the design of regulated Li^+ transport channels. One approach to exploit the 3D-connected pores and channels is to fill the pores with lithium salts and solvents or ionic liquids (ILs) containing both the charge carrier and ion-conducting media. In such cases, a charge-neutral MOF (Fig. 1a) is soaked in a liquid electrolyte where the framework exhibits weak or no interactions with

* Corresponding authors.
E-mail addresses: tingzhenghou@sz.tsinghua.edu.cn (T. Hou), wentaoxu@g.harvard.edu (W. Xu).

https://doi.org/10.1016/j.jechem.2023.02.048

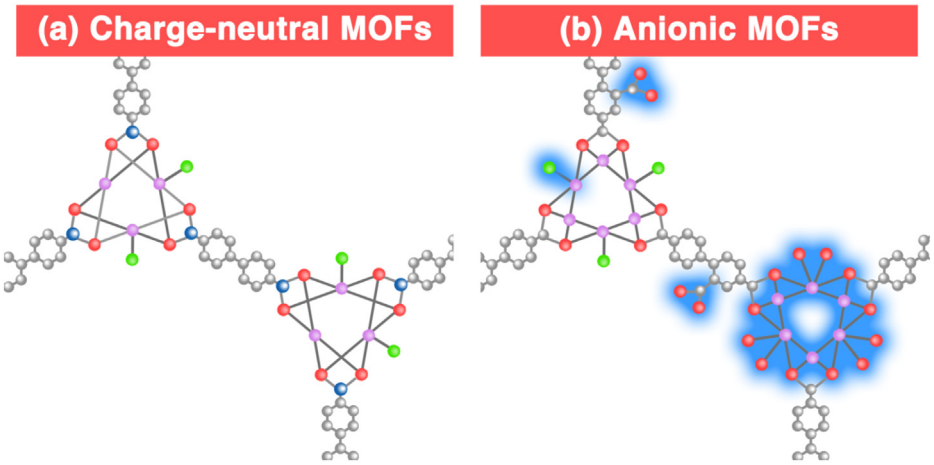

Fig. 1. Illustration of two types of metal–organic frameworks (MOFs) that have been utilized as Li^+-conducting solid matrices. (a) Charge-neutral MOFs. (b) Anionic MOFs with fixed negative charges. The sticks and balls denote the MOFs, while the diffused blue color denotes the negative charges.

the solvated anions/cations, and almost play a role as pure host materials [19]. While incorporating/encapsulating liquid electrolytes into the MOFs host can achieve high ionic conductivities (on the level of 10^{-4} S cm^{-1}, Ref. [19]), Li^+ transference numbers generally would not show any improvement compared with pristine liquid electrolytes (about 0.4) [22]. Additionally, considering that the external lithium salts that fill the intergranular cavities also contribute to the ionic conductivity, the intrinsic ionic conductivity contributed from lithium transport within the MOFs matrix remains questionable [22]. Another approach is to directly graft fixed negative charges on MOFs (Fig. 1b) so that Li^+ can be loaded as the charge balancing cation to create a single-ion conductor. By immobilizing the negative charge, high cation transference numbers (over 0.6) and suppressed polarization effect can be achieved [18]. Herein, in view of these superior features, we focus on discussing the latter anionic type of frameworks for the application of Li^+ electrolytes.

With relatively large pore sizes (ranging from 3 to 100 Å, Ref. [28,29]) in MOFs, the distance between neighboring Li^+ sites in the anionic MOFs matrix (about 2–10 Å, Ref. [30–33]) is typically larger than that in inorganic solid-state electrolytes (for example, Li garnet and other SICs have partially occupied, disordered Li sites within a short distance of less than 2 Å, Ref. [34]), leading to a high activation energy and a poor Li^+ conductivity for the pristine anionic MOFs at room temperature. Therefore, loading organic solvents into pores is generally required to help dissociate Li^+ from its countercharged binding sites and activate the ion transport. Consequently, the categorization of the anionic MOF-based composites as solid-state electrolytes has been inherently ambiguous. In fact, the terminology solid-state electrolytes are shared for both all-solid-state electrolytes and quasi-solid-state electrolytes [35]. The majority of research on MOF-based electrolytes does not further distinguish the terms, partially because MOF-based electrolytes behave more similarly to a solid from a rheological point of view. However, as the solvent contents in most MOF-based electrolytes are approximately 40% to 55% of the total weight [36], the solvent is deemed to offer essential functionality in Li^+ conduction. Therefore, the materials are suggested to be rigorously categorized as MOF-based quasi-solid-state electrolytes (MOF-QSSEs), which is a class of composite compounds consisting of a liquid electrolyte and a solid matrix [35].

Three strategies have been utilized for designing anionic MOF-QSSEs. First, immobilization of anions to coordinatively unsaturated open metal sites (OMSs) in charge-neutral frameworks (Fig. 2a). In 2011, Wiers et al. [17] first reported a prototype MOF-QSSEs by grafting LiO^iPr into Mg-MOF-74 (Mg_2(1,4-dioxido-2,5-benzenedicarboxylate)) through the coordination of isopropoxide anions to unsaturated Mg^{2+} sites. A conductivity of 1.2×10^{-5} S cm^{-1} was obtained with no additional salts. Other anions in Li salts or ILs, including $LiBF_4$ [37], LiTFSI (Lithium bis(trifluoromethanesulfonyl)imide) [38], LiO^tBu [39], and $LiClO_4$ [40], have also been reported to coordinate with OMSs. When anions are fully or partially trapped by OMSs through electrostatic interactions, Li^+ is expected to act as the predominant mobile charge carrier, fulfilling a maximized Li^+ transference number. However, the inevitable competition between anions and nucleophilic solvent molecules for OMSs in charge-neutral frameworks leads to the partial detachment of anions from the framework and thus to the contribution of anion mobility to the measured ionic conductivity. As a result, while the transference number of this type is higher than its corresponding liquid electrolyte with similar salts and solvents, the measured over 0.7 has not been reported [24]. The second strategy is to covalently link negatively charged constituents on framework backbones (Fig. 2b). One synesthetic approach is to utilize building blocks with acidic functional groups (phosphonate, sulfonate, carboxylate, etc.) that do not participate in reticulation [30,31,41]. Then, Li^+ can be introduced through the ion exchange with protons. Since acidic groups are often chemically/physiochemically active in binding metal ions, sophisticated or cautiously designed processes are required to guarantee that these acidic groups remain intact after the MOF crystallization. Another approach is to link functional groups on MOF linkers post-synthetically [42–44]. By installing the functional groups in a separate step after building the MOF, one can expect a simpler process and a wider chemical and topological selection. Zhu et al. [45] reported an anionic MOF (UiOLiTFSI) formed from covalent linking $TFSI^-$ and the amino groups of UiO-66-NH_2, which exhibited a high ionic conductivity (2.07×10^{-4} S cm^{-1} at 25 °C), a low activation energy of 0.31 eV, a wide electrochemical window up to 4.52 V, as well as a high Li^+ transference number of 0.84. The $LiFePO_4$|UiOLiTFSI + PVDF|Li full battery delivered an excellent cycling performance with a capacity of 147.7 mA h g^{-1} after 100 cycles at room temperature at 0.2 C (97.2% to the initial capacity of 152 mA h g^{-1}). The third strategy is to build intrinsically anionic frameworks (Fig. 2c). In intrinsically anionic frameworks, the Li^+ conductivity depends on the overall charge, as well as the chemical identity of the charged species. Conventional building units of MOFs and COFs carry no more than one charge, thus limiting the charge density of the framework [46,47]. Xu et al. reported an intrinsically anionic framework with a 3-fold interpenetration, ter-

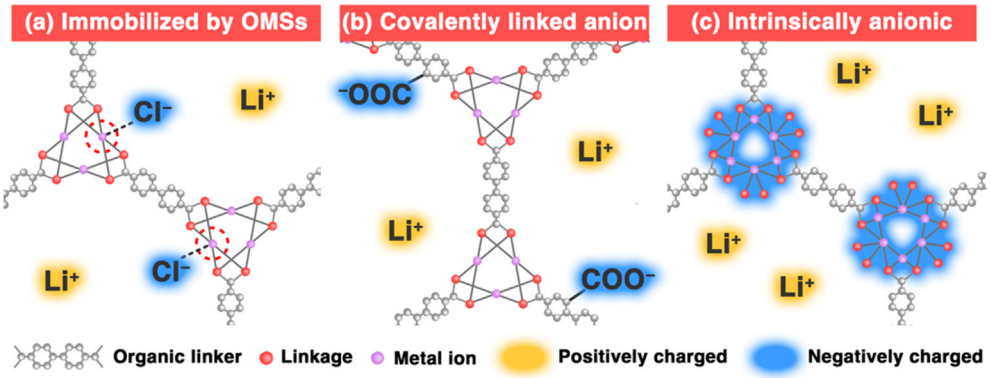

Fig. 2. Illustration of design strategies of anionic metal–organic frameworks based quasi-solid-state electrolytes (anionic MOF-QSSEs) by (a) immobilizing anions to open metal sites (OMSs) in charge-neutral frameworks, (b) covalently linking negatively charged constituents on framework backbones, and (c) building intrinsically anionic framework.

med MOF-688, constructed from highly charged Anderson-type polyoxometalates (POMs) [48]. MOF-688 exhibits high ionic conductivity (3.4×10^{-4} S cm^{-1} at 20 °C), a high transference number (t_{Li+} = 0.87), and low interfacial resistance (353 Ω) against metallic lithium. With a practical current density of 0.2 C, the LiFePO4|MOF-688|Li full cell achieved a capacity of 120 mA h g^{-1} after 200 cycles, representing 96% of the initial capacity and 92% of the capacity of the 10th cycle. Overall, given the diversity of structure, composition, and design strategy, it is important to understand the underlying structure–function relationship in order to rationally design anionic MOF-QSSEs.

2. How electrolytes transport Li+: anionic MOF-QSSEs vs others

Before diving into the detailed design principles and advantages of anionic MOF-QSSEs, we compare the materials with several other well-studied electrolyte systems, especially on their ionic conduction mechanism. The corresponding differences would provide insights into why anionic MOFs could be a suitable and promising choice as an electrolyte matrix.

2.1. Super-ionic conductors

Super-ionic conductor materials have shown several orders of magnitude higher ionic conductivity than typical solids [49]. Super-ionic conduction is known to be activated at high Li$^+$ concentrations and in specific mobile ion sublattice configurations achieved through materials doping [49]. For example, $Li_{10}GeP_2S_{12}$ (LGPS) [52], $Li_7P_3S_{11}$ (LPS) [53], lithium garnet (for example, $Li_7La_3Zr_2O_{12}$ (LLZO)) [54–56], and Li$^+$-conducting NASICON (for example, $Li_{1.5}Al_{0.5}Ge_{1.5}P_3O_{12}$ (LAGP)) [57,58], achieve high Li ionic conductivity, ~1–10 mS cm^{-1} at room temperature (RT), and low activation energy, ~0.2–0.3 eV. At low Li$^+$ concentrations, Li$^+$ diffusion occurs through isolated ion hopping so that the energy landscape of a single Li$^+$ along the migration channel passes through a high-energy transition state, which leads to a high diffusion barrier. Instead, at high concentrations, Li$^+$ diffusion in superionic conductors proceeds through concerted migrations (or knock-off mechanism) of multiple ions with low energy barriers (Fig. 3a). The concerted jump of Li$^+$, where the jump event of one Li$^+$ is affected by the jump of a different Li$^+$, can take up a non-negligible percentage of all the jump events. Modifying the percentage of correlated jump can tune the activation energy of ion diffusion and significantly improve ionic conductivity. Beyond the concerted motion, a paddle-wheel effect rising from cluster-ion rotation has been proposed to promote Li$^+$ conduction by lowering the activation barrier [59]. In addition, it was reported that the local distortions introduced into high-entropy materials can give rise to an overlapping distribution of site energies for the Li$^+$ so that it can percolate with even lower activation energy [60]. As a comparison, the concerted/correlated ion diffusion is insignificant in anionic MOF-QSSEs at room temperature, as analyzed using molecular dynamics simulations and the Onsager transport theory [33]. Another main advantage of utilizing dense solid-state electrolytes is the high mechanical strength, which can significantly suppress Li dendrites formation. However, a trade-off exists where high elastic modulus typically leads to poor surface adhesion and high interfacial resistance, restricting the full battery cycling life [16].

2.2. Gel-polymer electrolytes

Gel-polymer electrolytes (GPEs) are the most common QSSEs [61], among which poly(ethylene oxide) (PEO) has been the dominant polymer matrix for the development of the materials [62–65]. GPEs were proposed to improve the limited ionic conductivity of solid polymer electrolytes (10^{-8}–10^{-5} S cm^{-1}), and satisfactory conductivity values (up to 10^{-2} S cm^{-1} at 25 °C) can be achieved with a high content of liquid plasticizers in GPEs [66]. Taking into account that most electrolytes based on PEO are not crosslinked, and those that are crosslinked do not possess permanent pores [67], their structural composition differs substantially from that of metal–organic frameworks (MOFs). As a result, with intrinsic low structural rigidity, PEO in GPEs further loses mechanical strength when infiltrated and plasticized by organic solvents [31,68]. In comparison, the elastic modulus of MOF crystals increases as their pores are filled [61,69]. In addition, non-crystalline GPEs will inevitably introduce uneven Li$^+$ distribution and unordered diffusion channels within the electrolyte matrix. The inhomogeneity will lead to the non-uniform distribution of Li$^+$, which is considered detrimental to the anode operation [61].

2.3. Polyelectrolytes

As another type of polymer-based electrolytes, polyelectrolyte solutions have also been proposed as alternatives to conventional solid-state single-ion conductors with conductivities on the order of 10^{-4}–10^{-3} S cm^{-1} [50]. Analogous to anionic MOF-QSSEs, polyelectrolytes consist of a lithium-neutralized polyanion dissolved in a nonaqueous solvent [70]. Intuitively, the sluggish motion of polyanions could have led to the dominancy of Li$^+$ transport and a high Li$^+$ transference number if the ions were well separated. However, coarse-grained molecular dynamics simulations have shown proof that the transference number is substantially lower

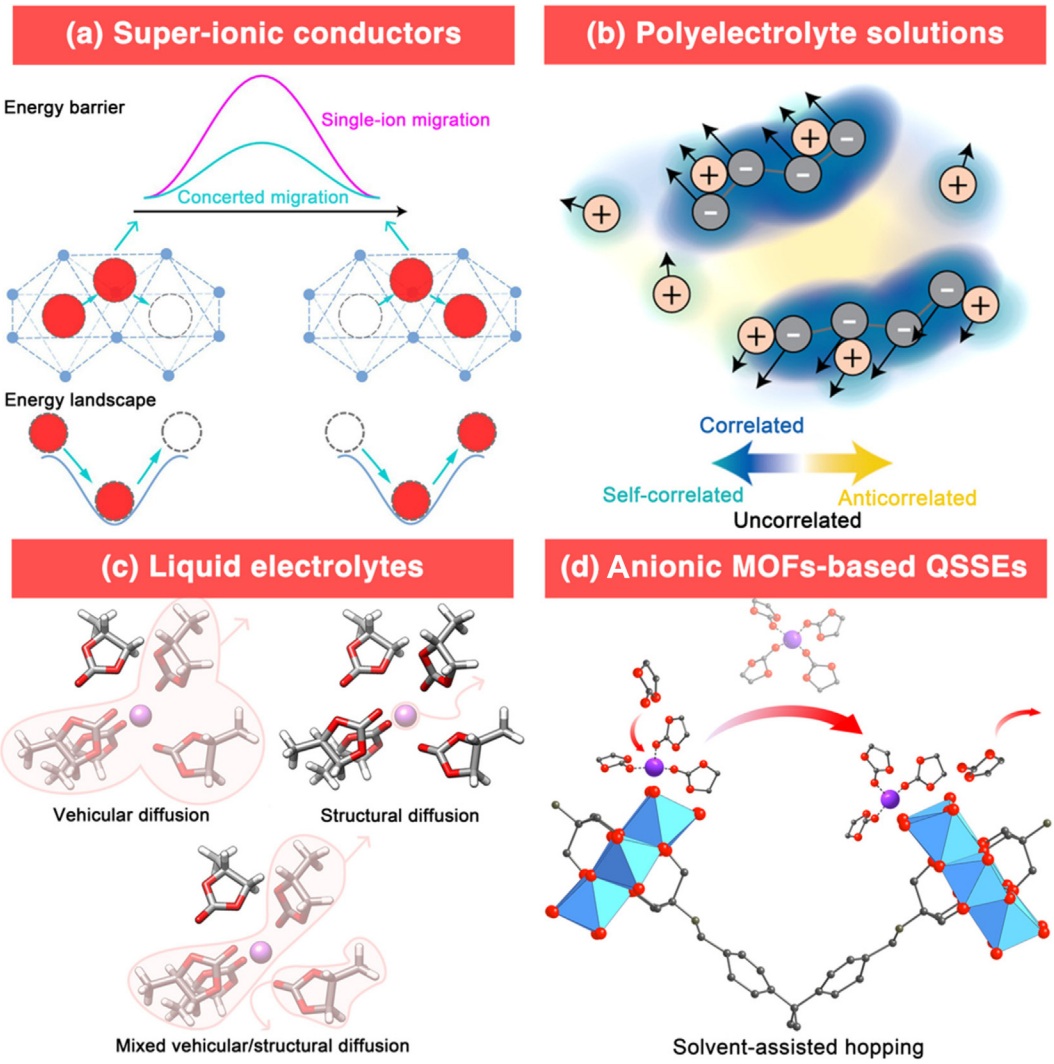

Fig. 3. (a) Schematic illustration of single-ion migration versus multi-ion concerted migration in solid-state fast ion conductors [49]. (b) Schematic illustration of anion–anion, cation–anion, and cation–cation correlations in polyelectrolyte solutions, adapted with permission from Ref [50]. Copyright 2020 American Chemical Society. (c) Illustration of Li^+ diffusion of vehicular quality, structural quality, and a mix of structural and vehicular quality in liquid electrolytes, adapted with permission from [51]. Copyright 2019 American Chemical Society. (d) Illustration of solvent-assisted hopping in anionic MOF-QSSEs [33].

than expected due to the presence of strong anion–anion and cation–anion correlations (Fig. 3b). None of the theoretically investigated polyelectrolyte solutions achieve t_{Li+} greater than that of the conventional liquid electrolyte [50].

2.4. Nonaqueous liquid electrolytes

Nonaqueous Liquid electrolytes are the most conventional media for Li transport in LIBs/LMBs [71–73]. A most simple setup is to dissolve a Li salt in an organic solvent, where the Li salt dissociated in the electrolyte, fully or partially, to enable Li^+ transport (typically 10^{-3}–10^{-2} S cm^{-1}, Ref. [72]). Fig. 3(c) shows the Li^+ transport regimes [51]. At lower concentrations, Li^+ diffuses appreciably with its coordinating solvents under the vehicular transport regime. As the concentration increases, the structural diffusion (also referred to as Grotthuss-type, Ref. [74–76]) of Li^+ may become the main transport mode, where the neighboring species do not diffuse together by any appreciable amount. For example, the neighboring solvents are frequently exchanged as the solvated species diffuses with its shell or the species undergoes some type of hopping or Grotthuss-type mechanism. At an intermediate concentration lever, a mix of structural and vehicular-type diffusion occurs, where a solvent is lost as Li^+ diffuses a distance comparable to the size of a solvation shell, while the remaining fraction of the solvation shell diffuses as a single kinetic entity. With this mixed ionic conduction mechanism, Li^+ transport can be greatly affected by the local environment and interfacial conditions. The susceptibility will result in uneven transport of Li^+, causing Li^+ concentration gradients and battery polarization, which further leads to the growth of dendrites. In fact, while only Li^+ mobility is desired, liquid electrolytes allow the diffusion of both anions and Li^+. On one hand, the undesired anion concentration gradient would aggravate the polarization effect and even cause parasitic reactions [77–79]. On the other hand, the correlated diffusion of anions and Li^+ will significantly decrease the total Li^+ conductivity. Further, even though it is feasible to physically tune the Li^+ transport regime and enhance Li^+ conductivity with different electrolyte formulas, it is still not possible to rationally design chemically passivating liquid electrolytes for Li metal anode materials.

2.5. Anionic MOF-QSSEs

Determining the ionic conduction mechanism is not trivial for anionic MOF-QSSEs, especially given the characterization challenges associated with solvation structures and transport properties within the nanopores [80–82]. Some of the pioneering

studies have described the Li^+ conduction in anionic MOFs as a simple hopping mechanism between lithium binding sites. For example, Wiers et al. [17] "anticipated" a conduction mechanism where Li^+ cations hop from site to site. Yuan et al. [32] suggested that the charge is transported by coordinated hopping of Li^+ between the perchlorate groups in Cu-MOF-74 through quantum mechanical calculation. However, these studies, as well as the work by Park et al. [37], did not consider the critical role of solvent molecules in the Li^+ conduction in MOFs. In particular, previous reports show that neglecting the solvent makes it impossible to explain the large conductivity difference (at least three orders of magnitude, Ref. [83]) between the dried and solvated MOF-based electrolytes. Recently, through solid-state NMR characterizations, Zettl et al. [31] demonstrated that the conduction mechanism of MIL-121/Li + SE follows correlated dynamics influenced by the solvent molecules and the MOF structure at low temperature, and approximately independent (uncorrelated) cation dynamics of the Li^+ residing near the immobilized anionic functional groups at high temperature. However, the underlying information on how the solvent molecules facilitate the diffusion of Li^+ remains unclear. For example, whether Li^+ is fully solvated and dissociated from the framework, or if they are partially solvated by the solvent molecules. Recently, Hou and Xu et al. [33] developed a theoretical model to further distinguish the influence of the anionic framework and the solvent molecules on Li^+ conduction. Using classical molecular dynamics in conjunction with quantum chemistry and grand canonical Monte Carlo methods, the solvent-assisted hopping mechanism is identified as the dominant pathway for Li^+ conduction in an intrinsically anionic MOF-QSSEs material, revealing the critical role of solvent molecules at an atomistic level in MOF-based electrolytes (Fig. 3d).

3. Benefits of using anionic MOF-QSSEs as electrolytes for LMBs

The nature of MOFs offers several advantages to anionic MOF-QSSEs as promising candidates for LMBs electrolytes. First, MOFs have tunable pores and ordered channels through which lithium ions can be transported. Designable porous structures (i.e., pore shape, pore size, and pore polarity) can enhance cation diffusion and suppress undesired side reactions. A periodic crystalline structure with ordered channels enables well-defined pathways for ion transfer and uniform cation plating/stripping processes, which suppresses dendrite growth and improves cycling stability. In addition, MOFs possess an ultra-high surface area, which provides a sufficiently high density of Li^+ binding sites and transport pathways, promoting ion transport dynamics. Moreover, we emphasize that compared to other types of QSSEs (e.g., GPEs) where the solvent swells and expands the polymer matrix, the solvent trapped inside the pores does not compromise the mechanical properties of the MOFs [31,33]. For example, the theoretical bulk moduli (Voigt average) of the intrinsically anionic MOF-688 is 6.7 GPa, which is one to two orders of magnitude higher than that of PEO-based GPEs [33].

Another aspect of benefits arises from the periodicity of anionic MOF-QSSEs, i.e., anionic sites are uniformly distributed on the backbone of the MOFs. In principle, the immobilization of anions onto the framework promotes the ionic conduction of Li^+ by preventing the migration and accumulation of anions. This ion transport regime greatly reduces the polarization effect as observed in liquid electrolytes and restricts parasitic reactions of anions on the electrode. Especially, for intrinsically anionic MOF-QSSEs, the anionic charge with a long-range order encourages the homogeneous distribution of the charge-balancing Li^+ throughout the host matrix while minimizing the incorporation of mobile, exogenous species that are typically introduced by coordination with OMSs or post-synthetic process [18].

4. Tuning chemical and topological characters to increase Li+ conductivity

4.1. Pore size

In general, the amount of solvent loading increases along with the size of the pores. While fewer water molecules are favored in proton-conducting MOFs to minimize hydrogen bonds [87], the conduction of Li^+ typically requires adequate solvent molecules to facilitate the solvation of Li^+ [9]. To increase the pore size, one straightforward strategy is to use longer organic linkers. For example, Shen et al. [84] compared the ionic conductivity of two MOFs materials, UIO-66 and UIO-67, as QSSEs hosts. UiO-66 ($Zr_6O_4(OH)_4(BDC)_6$, BDC = 1,4-dicarboxylate) and UiO-67 ($Zr_6O_4(OH)_4(BPDC)_6$, BPDC = biphenyl-4,4′-dicarboxylate) shares the same topology structure and OMSs by bridging the $Zr_6O_4(OH)_4$ cornerstones, but with different organic linkers (Fig. 4a). UiO-67 with a longer BPDC linker exhibits larger pore size (two types of continuous pores: 12 Å and 16 Å) than that of UiO-66 (7.5 Å and 12 Å). A more than three times higher conductivity was observed for the UIO-67 based QSSEs (6.5×10^{-4} S cm^{-1}) compared to the UIO-66 based (1.8×10^{-4} S cm^{-1}). The higher Li^+ conductivity observed in UiO-67 was attributed to the larger pore size being able to accommodate a higher extent of solvation around the Li^+ ions, which enhances mobility. A lower activation energy was obtained in UiO-67 (0.12 eV) versus UiO-66 as well (0.21 eV).

Another approach to open large pores is to tune the degree of interpenetration of MOFs. When long organic links are used in building certain nets, especially those of primitive cubic topology, the resulting frameworks are entangled over the entire crystal structure. In other words, two or more independent frameworks are found completely interpenetrated to fill what otherwise would have been large pores [88]. To actually synthesize less interpenetrated MOFs, large and appropriately matching template guests or cations are required to support the reticulation of organic and inorganic building blocks. Although the strategy has not been experimentally validated, atomistic simulations have shown that for a three-fold interpenetrated anionic MOF-688 material, its hypothesized non-interpenetrating counterpart is expected to achieve 6–8 times better theoretical ionic conductivity (Fig. 4b), while retaining about 1/3 of the theoretical bulk modulus of MOF-688.

4.2. Density and ionic strength of anionic species

First of all, the pore size and the density of immobilized anionic species should be properly matched. In other words, there should be enough binding sites for Li^+ if transported by the hopping mechanism, but at the same time charged species should not be too concentrated. Moreover, if the charge on a certain immobilized anionic group is strongly localized, then Li^+ is expected to be more tightly confined. The strong binding between Li^+ ions and the framework may cause less favorable Li^+ hopping, which in turn, may decrease the mobility and ionic conductivity. Therefore, the introduction of more distributed local charges on negatively charged groups is anticipated to facilitate weaker binding with Li^+ ions and enhance Li^+ motion. For example, Park et al. [37] reported the utilization of MIT-20 ($(((CH3)_2NH_2)[Cu_2Cl_3BTDD]\cdot(DMF)_4(H_2O)_{4.5}$, H_2BTDD = bis(1H-1,2,3-triazolo[4,5-*b*],[4′,5′-*i*])dibenzo-[1,4]dioxin) to synthesize anionic MOFs-QSSEs. A series of LiCl, LiBr, and $LiBF_4$ salts with an increasing softness of the anion was grafted into MIT-20 by coordinating the anions with OMSs (Fig. 4c). The Li^+ conductivity increases as the anion changes from the most charge-localized Cl^- (1.3×10^{-5} S cm^{-1}) to the most charge-distributed BF_4^- (4.8×10^{-4} S cm^{-1}), indicating the effect of anion softness on Li^+

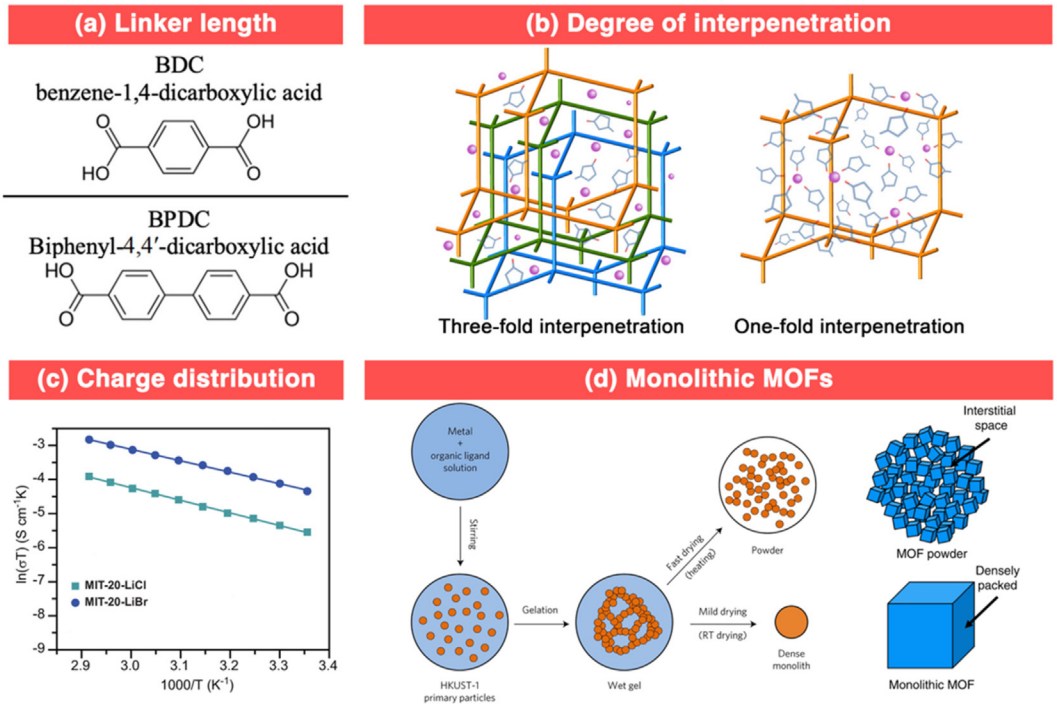

Fig. 4. (a) BDC (1,4-dicarboxylate) and BPDC (biphenyl-4,4′-dicarboxylate) linkers with different lengths used in UiO-66 and UiO-67, respectively, adapted with permission from Ref. [84]. Copyright 2018 WILEY-VCH. (b) Schemes of MOF-688 QSSEs with three-fold and proposed one-fold interpenetrating structures [33]. (c) Ionic conductivities as a function of temperature in the range of 25 to 70 °C for MIT-20-LiCl and MIT-20-LiBr, adapted with permission from Ref. [37]. Copyright 2017 American Chemical Society. (d) Schematic representation of monolithic and powder MOF synthesis [85]. The left panel is adapted from Ref. [86] with permissions. Copyright 2017 Nature Publishing Group.

mobility. However, it should be noted that the Li^+ transference number for MOFs with LiCl can go as high as 0.69, while MOFs with LiBr showed a lower transference number of 0.34, revealing the weaker strength between soft anions with OMSs and weakened immobilization of anionic charges on MOFs [89].

In fact, the binding strength of OMSs and anions could be further tuned by changing the type of OMSs. For example, in the same study by Shen et al. [84], QSSEs based on a series of MIL-100 MOFs with varying OMSs were also investigated. The MOFs had the same structure but with varying metal ions (Al^{3+}, Fe^{3+}, Cr^{3+}) as OMSs. The obtained ionic conductivity was in good agreement with the trend of Lewis acidity of the OMSs (Al > Fe > Cr). The stronger acidity of Al^{3+} with a stronger acidity compared to Fe^{3+} and Cr^{3+} can exhibit stronger interactions with the anions, thus weakening the ion-pairing strength between Li^+ and ClO_4^-, which enables fast conduction of Li^+ ions. In contrast, for intrinsically anionic MOF-688, changing the type of center metal ions from Mn^{3+} to Al^{3+} has been reported to be ineffective in tuning the ionic conductivity. The difference originates from the fact that center metal ions inside the POM cluster with the same valency exhibit minor influence on the surface charge distribution, while for OMSs, the metal ions are exposed. Therefore, changing the valency of these center metal ions is suggested as a possible approach to tune the ionic strength of the anionic POM cluster [90]. For anionic MOF-QSSEs with covalently linked anionic functional groups, incorporating softer acidic groups has also been speculated to be effective in mitigating the strong binding between the anionic group and Li^+, for example, by substituting carboxylic acid groups (R-COOH) with monothioic acid groups (R-COSH) [22].

4.3. Grain boundary

Anionic MOF-QSSEs are generally prepared by pressing single crystalline or polycrystalline MOFs into pellets, where abundant voids are expected between grains [26]. In some cases, the density of MOF pellets can only reach about 75% of their ideal density, suggesting a high intergranular volume [91]. While the metal clusters and organic linkers are connected by strong coordination or covalent bonds within the crystal, the grains are connected by weak interactions. As a result, the grain boundary becomes the mechanically weakest point of anionic MOF-QSSEs, where lithium dendrites can easily penetrate [92]. Furthermore, these gaps and voids, which block the pathways of Li+ transport, are also anticipated to be detrimental to ion transport in anionic MOF-QSSEs [93]. To what extent these gaps and voids contribute to ionic conductivity will require further research to understand.

A promising route to eliminate grain boundaries is to synthesize monolithic MOFs (Fig. 4d). It was reported that through a sol–gel process, HKUST-1 nanoparticles can be connected into monolithic MOFs that are free of boundary or interphase between primary particles [86]. The obtained monolithic MOFs exhibited a hardness 130% greater than the polycrystalline HKUST-1 film. Gas adsorption measurement also showed that the diffusion pathway was not blocked in the monolithic. A similar process can be applied to other MOFs such as ZIF-4, ZIF-8, and UiO-66 [85], where the hardness of the MOF monolith is comparable to that of their single crystalline counterpart. Although this strategy has not been applied to anionic MOFs, it sheds light on a possible research agenda to construct anionic MOF-QSSEs with higher ionic conductivity and mechanical properties.

5. Outlooks

The central role of anionic frameworks in modulating anionic MOF-QSSEs has long been spotlighted in the area. However, the significance of solvent molecules in facilitating Li^+ transport has not been fully recognized until recently. In particular, few studies have investigated the influence of solvents with varying solvating power on the ionic conductivity as well as the ionic conduction mechanism. Taking the lesson from liquid electrolyte systems

[94], the solvation ability of various electrolyte solvents is at least equally important as the ionic strength of immobilized anionic species for regulating Li^+ transport. Another missing but important fragment in current studies is the electrochemical cycling performance of anionic MOF-QSSEs in practical half or full cell setups. It should be noted that even for all-solid-state electrolytes, a very thin SEI would be formed [95]. For anionic MOF-QSSEs, reduction reactions of the organic solvent are deemed to occur during initial cycles. Framework backbones or functional groups are also potentially reactive or unstable within the operating electrochemical window. The interface interactions and reactions should be meticulously considered in the design of anionic MOF-QSSEs [96]. Forming an optimal SEI layer that can passivate the lithium anode surface against further side reactions while facilitating ion transport should be the golden standard for developing any novel electrolytes [97].

On a larger scale, the molding process will play a more important role in the future development or preparation of anionic MOF-QSSEs. So far, pressed pellets of MOF powders are adequate for prototype coin cells. However, the fragility and poor processability of the pellet make them unsuitable for batteries on a larger scale. Considering that binders can potentially block the ion diffusion pathway, technologies that can transform MOF powder into processable, binder-free thin films are of particular interest. Solvent-free hot-pressing techniques have been used to fabricate various types of large-area MOF films [98], while 3D printing [99] techniques were used to fabricate MOF monoliths with complicated 3D structures. We anticipate that these technologies will be helpful in the development of anionic MOF-QSSEs.

In a broader context, MOFs can act as functionalized fillers or host materials for different SSE systems for LMBs. However, the detailed ion transport mechanisms, as well as the exact role of MOFs are still unclear [19]. A more careful study of the anionic MOF-QSSEs as a prototype material is expected to provide insights into the role of MOFs in a more complicated composite electrolyte. Beyond lithium batteries, anionic MOF-QSSEs have also been used in other novel energy storage systems [100]. For example, Ma et al. [101] synthesized anionic MOF-QSSEs containing third-period cations (Na^+, Mg^{2+}, and Al^{3+}) by soaking MOF frameworks with the perchlorate salts (1 M) in propylene carbonate. Fourier-transform infrared spectra show that the anions were immobilized inside the MOF scaffolds upon complexing with OMSs, allowing effective transport of the cations in the nano-porous channels with high conductivity (up to 10^{-3} S cm^{-1}) and low activation energy (down to 0.2 eV). This work has opened up new opportunities for exploring the tunability of anionic MOFs in accordance with the characteristics of different cations.

Finally, considering the ultra-high tunability of anionic MOF-QSSEs, we anticipate that high-throughput calculations and machine learning methods can help screen promising candidates of novel materials within this type. For example, computational screening methods based on periodic density functional theory have been used for investigating O_2 and N_2 adsorption at the coordinatively unsaturated metal sites of several MOF families [102]. Moreover, databases hosting quantum mechanical properties for thousands of MOFs have been established [103]. The massive amount of data would help to build machine learning models that allow obtaining key properties of candidate MOFs for designing anionic MOF-QSSEs at a very low time and material cost, such as the charge distribution of anionic groups.

Declaration of competing interest

The authors declare that they have no known competing financial interests or personal relationships that could have appeared to influence the work reported in this paper.

Acknowledgments

We thank Dr. Lu Jiang for proofreading the manuscript. The work is financially supported by the Scientific Research Startup Funds from Tsinghua Shenzhen International Graduate School.

References

[1] T.-Z. Hou, X. Chen, H.-J. Peng, J.-Q. Huang, B.-Q. Li, Q. Zhang, B. Li, Small 12 (2016) 3283–3291.
[2] Z. Yuan, H.-J. Peng, T.-Z. Hou, J.-Q. Huang, C.-M. Chen, D.-W. Wang, X.-B. Cheng, F. Wei, Q. Zhang, Nano Lett. 16 (2016) 519–527.
[3] X. Chen, T. Hou, K.A. Persson, Q. Zhang, Mater. Today 22 (2019) 142–158.
[4] X.-B. Cheng, R. Zhang, C.-Z. Zhao, Q. Zhang, Chem. Rev. 117 (2017) 10403–10473.
[5] D. Lin, Y. Liu, Y. Cui, Nat. Nanotechnol. 12 (2017) 194–206.
[6] Y.-Y. Wang, X.-Q. Zhang, M.-Y. Zhou, J.-Q. Huang, Nano Res. Energy 2 (2022) e9120046.
[7] W. Xu, J. Wang, F. Ding, X. Chen, E. Nasybulin, Y. Zhang, J.-G. Zhang, Energ. Environ. Sci. 7 (2014) 513–537.
[8] M.-Y. Zhou, X.-Q. Ding, J.-F. Ding, L.-P. Hou, P. Shi, J. Xie, B.-Q. Li, J.-Q. Huang, X.-Q. Zhang, Q. Zhang, Joule 6 (2022) 2122–2137.
[9] S.-Y. Sun, N. Yao, C.-B. Jin, J. Xie, X.-Y. Li, M.-Y. Zhou, X. Chen, B.-Q. Li, X.-Q. Zhang, Q. Zhang, Angew. Chem. Int. Ed. 61 (2022) e202208743.
[10] T. Hou, X. Chen, L. Jiang, C. Tang, J. Electrochem. 28 (2022) 2219007.
[11] Y. Sun, N. Liu, Y. Cui, Nat. Energy 1 (2016) 16071.
[12] T. Hou, G. Yang, N.N. Rajput, J. Self, S.-W. Park, J. Nanda, K.A. Persson, Nano Energy 64 (2019).
[13] R. Chen, W. Qu, X. Guo, L. Li, F. Wu, Mater. Horiz. 3 (2016) 487–516.
[14] L. Fan, S. Wei, S. Li, Q. Li, Y. Lu, Adv. Energy Mater. 8 (2018) 1702657.
[15] X.-B. Cheng, C.-Z. Zhao, Y.-X. Yao, H. Liu, Q. Zhang, Chem. 5 (2019) 74–96.
[16] K. Qin, K. Holguin, M. Mohammadiroudbari, J. Huang, E.Y.S. Kim, R. Hall, C. Luo, Adv. Funct. Mater. 31 (2021) 2009694.
[17] B.M. Wiers, M.L. Foo, N.P. Balsara, J.R. Long, J. Am. Chem. Soc. 133 (2011) 14522–14525.
[18] E.M. Miner, M. Dinca, Philos. Trans. R. Soc. A 377 (2019) 20180225.
[19] R. Zhao, Y. Wu, Z. Liang, L. Gao, W. Xia, Y. Zhao, R. Zou, Energ. Environ. Sci. 13 (2020) 2386–2403.
[20] W.-H. Huang, X.-M. Li, X.-F. Yang, X.-X. Zhang, H.-H. Wang, H. Wang, Mater. Chem. Front. 5 (2021) 3593–3613.
[21] T. Chen, S. Chen, Y. Chen, M. Zhao, D. Losic, S. Zhang, Mater. Chem. Front. 5 (2021) 1771–1794.
[22] R.A. Kharod, J.L. Andrews, M. Dincă, Annu. Rev. Mat. Res. 52 (2022) 103–128.
[23] S. Jiang, T. Lv, Y. Peng, H. Pang, Adv. Sci. (2023), https://doi.org/10.1002/advs.202206887.
[24] T. Wei, Z. Wang, Q. Zhang, Y. Zhou, C. Sun, M. Wang, Y. Liu, S. Wang, Z. Yu, X. Qiu, S. Xu, S. Qin, CrstEngComm 24 (2022) 5014–5030.
[25] X. Hu, Q. Liu, K. Lin, C. Han, B. Li, J. Mater. Chem. A 9 (2021) 20837–20856.
[26] W. Xue, C.D. Sewell, Q. Zhou, Z. Lin, Angew. Chem. Int. Ed. 61 (2022) e202206512.
[27] H. Furukawa, K.E. Cordova, M. O'Keeffe, O.M. Yaghi, Science 341 (2013) 1230444.
[28] Y. Cui, B. Li, H. He, W. Zhou, B. Chen, G. Qian, Acc. Chem. Res. 49 (2016) 483–493.
[29] W. Xuan, C. Zhu, Y. Liu, Y. Cui, Chem. Soc. Rev. 41 (2012) 1677–1695.
[30] L. Tian, X. Xu, M. Liu, Z. Liu, Z. Liu, Langmuir 37 (2021) 3922–3928.
[31] R. Zettl, S. Lunghammer, B. Gadermaier, A. Boulaoued, P. Johansson, H.M.R. Wilkening, I. Hanzu, Adv. Energy Mater. 11 (2021) 2003542.
[32] S. Yuan, J.-L. Bao, J. Wei, Y. Xia, D.G. Truhlar, Y. Wang, Energ. Environ. Sci. 12 (2019) 2741–2750.
[33] T. Hou, W. Xu, X. Pei, L. Jiang, O.M. Yaghi, K.A. Persson, J. Am. Chem. Soc. 144 (2022) 13446–13450.
[34] X. He, Q. Bai, Y. Liu, A.M. Nolan, C. Ling, Y. Mo, Adv. Energy Mater. 9 (2019) 1902078.
[35] X. Judez, M. Martinez-Ibañez, A. Santiago, M. Armand, H. Zhang, C. Li, J. Power Sources 438 (2019).
[36] M.L. Aubrey, R. Ameloot, B.M. Wiers, J.R. Long, Energ. Environ. Sci. 7 (2014) 667.
[37] S.S. Park, Y. Tulchinsky, M. Dinca, J. Am. Chem. Soc. 139 (2017) 13260–13263.
[38] R. Bouchet, S. Maria, R. Meziane, A. Aboulaich, L. Lienafa, J.P. Bonnet, T.N. Phan, D. Bertin, D. Gigmes, D. Devaux, R. Denoyel, M. Armand, Nat. Mater. 12 (2013) 452–457.
[39] R. Ameloot, M. Aubrey, B.M. Wiers, A.P. Gomora-Figueroa, S.N. Patel, N.P. Balsara, J.R. Long, Chem. Eur. J. 19 (2013) 5533–5536.
[40] A. Ulihin, V. Ponomareva, N. Uvarov, K. Kovalenko, V. Fedin, Ionics 26 (2020) 6167–6173.
[41] X. Duan, Y. Ouyang, Q. Zeng, S. Ma, Z. Kong, A. Chen, Z. He, T. Yang, Q. Zhang, Inorg. Chem. 60 (2021) 11032–11037.
[42] A.E. Baumann, D.A. Burns, J.C. Diaz, V.S. Thoi, ACS Appl. Mater. Interfaces 11 (2019) 2159–2167.
[43] H. Yang, B. Liu, J. Bright, S. Kasani, J. Yang, X. Zhang, N. Wu, ACS Appl. Energy Mater. 3 (2020) 4007–4013.
[44] P. Chiochan, X. Yu, M. Sawangphruk, A. Manthiram, Adv. Energy Mater. 10 (2020) 2001285.

[45] F. Zhu, H. Bao, X. Wu, Y. Tao, C. Qin, Z. Su, Z. Kang, ACS Appl. Mater. Interfaces 11 (2019) 43206–43213.
[46] H. Furukawa, N. Ko, Y.B. Go, N. Aratani, S.B. Choi, E. Choi, A.O. Yazaydin, R.Q. Snurr, M. O'Keeffe, J. Kim, O.M. Yaghi, Science 329 (2010) 424–428.
[47] W. Lu, Z. Wei, Z.Y. Gu, T.F. Liu, J. Park, J. Park, J. Tian, M. Zhang, Q. Zhang, T. Gentle 3rd, M. Bosch, H.C. Zhou, Chem. Soc. Rev. 43 (2014) 5561–5593.
[48] W. Xu, X. Pei, C.S. Diercks, H. Lyu, Z. Ji, O.M. Yaghi, J. Am. Chem. Soc. 141 (2019) 17522–17526.
[49] X. He, Y. Zhu, Y. Mo, Nat. Commun. 8 (2017) 15893.
[50] K.D. Fong, J. Self, B.D. McCloskey, K.A. Persson, Macromolecules 53 (2020) 9503–9512.
[51] J. Self, K.D. Fong, K.A. Persson, ACS Energy Lett. 4 (2019) 2843–2849.
[52] N. Kamaya, K. Homma, Y. Yamakawa, M. Hirayama, R. Kanno, M. Yonemura, T. Kamiyama, Y. Kato, S. Hama, K. Kawamoto, A. Mitsui, Nat. Mater. 10 (2011) 682–686.
[53] Y. Seino, T. Ota, K. Takada, A. Hayashi, M. Tatsumisago, Energ. Environ. Sci. 7 (2014) 627–631.
[54] R. Murugan, V. Thangadurai, W. Weppner, Angew. Chem. Int. Ed. 46 (2007) 7778–7781.
[55] K. Fu, Y. Gong, G.T. Hitz, D.W. McOwen, Y. Li, S. Xu, Y. Wen, L. Zhang, C. Wang, G. Pastel, J. Dai, B. Liu, H. Xie, Y. Yao, E.D. Wachsman, L. Hu, Energ. Environ. Sci. 10 (2017) 1568–1575.
[56] J. Zhu, X. Li, C. Wu, J. Gao, H. Xu, Y. Li, X. Guo, H. Li, W. Zhou, Angew. Chem. Int. Ed. 60 (2021) 3781–3790.
[57] Q. Liu, D. Zhou, D. Shanmukaraj, P. Li, F. Kang, B. Li, M. Armand, G. Wang, ACS Energy Lett. 5 (2020) 1456–1464.
[58] Y. Nikodimos, L.H. Abrha, H.H. Weldeyohannes, K.N. Shitaw, N.T. Temesgen, B. W. Olbasa, C.-J. Huang, S.-K. Jiang, C.-H. Wang, H.-S. Sheu, S.-H. Wu, W.-N. Su, C.-C. Yang, B.J. Hwang, J. Mater. Chem. A 8 (2020) 26055–26065.
[59] Y. Sun, B. Ouyang, Y. Wang, Y. Zhang, S. Sun, Z. Cai, V. Lacivita, Y. Guo, G. Ceder, Matter 5 (2022) 4379–4395.
[60] Y. Zeng, B. Ouyang, J. Liu, Y.W. Byeon, Z. Cai, L.J. Miara, Y. Wang, G. Ceder, Science 378 (2022) 1320–1324.
[61] A. Manuel Stephan, Eur. Polym. J. 42 (2006) 21–42.
[62] M. Moreno, R. Quijada, M.A. Santa Ana, E. Benavente, P. Gomez-Romero, G. González, Electrochim. Acta 58 (2011) 112–118.
[63] S. Klongkan, J. Pumchusak, Electrochim. Acta 161 (2015) 171–176.
[64] Z. Xue, D. He, X. Xie, J. Mater. Chem. A 3 (2015) 19218–19253.
[65] C.-Z. Zhao, Q. Zhao, X. Liu, J. Zheng, S. Stalin, Q. Zhang, L.A. Archer, Adv. Mater. 32 (2020) e1905629.
[66] D. Zhou, D. Shanmukaraj, A. Tkacheva, M. Armand, G. Wang, Chem. 5 (2019) 2326–2352.
[67] L. Tian, M. Wang, Y. Liu, Z. Su, B. Niu, Y. Zhang, P. Dong, D. Long, J. Power Sources 543 (2022).
[68] M. Zhu, J. Wu, Y. Wang, M. Song, L. Long, S.H. Siyal, X. Yang, G. Sui, J. Energy Chem. 37 (2019) 126–142.
[69] K. Yang, G. Zhou, Q. Xu, RSC Adv. 6 (2016) 37506–37514.
[70] K.D. Fong, J. Self, K.M. Diederichsen, B.M. Wood, B.D. McCloskey, K.A. Persson, ACS Cent. Sci. 5 (2019) 1250–1260.
[71] T. Hou, K.D. Fong, J. Wang, K.A. Persson, Chem. Sci. 12 (2021) 14740–14751.
[72] K. Xu, Chem. Rev. 104 (2004) 4303–4418.
[73] K. Xu, Chem. Rev. 114 (2014) 11503–11618.
[74] C.J.T. de Grotthuss, Ann. Chim. LVIII (1805) 54–74.
[75] I. Rubinstein, M. Bixon, E. Gileadi, J. Phys. Chem. 84 (1980) 715–721.
[76] N. Agmon, Chem. Phys. Lett. 244 (1995) 456–462.
[77] H.-L. Long, H.-J. Peng, Chin. Chem. Lett. 34 (2023).
[78] H.-J. Peng, J.-Q. Huang, X.-Y. Liu, X.-B. Cheng, W.-T. Xu, C.-Z. Zhao, F. Wei, Q. Zhang, J. Am. Chem. Soc. 139 (2017) 8458–8466.
[79] X. Liu, H.-J. Peng, B.-Q. Li, X. Chen, Z. Li, J.-Q. Huang, Q. Zhang, Angew. Chem. Int. Ed. 61 (2022) e202214037.
[80] M. Cronau, M. Szabo, C. König, T.B. Wassermann, B. Roling, ACS Energy Lett. 6 (2021) 3072–3077.
[81] J.M. Winand, J. Depireux, Europhys. Lett. 8 (1989) 447–452.
[82] Y. Lu, C.-Z. Zhao, J.-Q. Huang, Q. Zhang, Joule 6 (2022) 1172–1198.
[83] J. Brus, J. Czernek, M. Urbanova, J. Rohlicek, T. Plechacek, ACS Appl. Mater. Interfaces 12 (2020) 47447–47456.
[84] L. Shen, H.B. Wu, F. Liu, J.L. Brosmer, G. Shen, X. Wang, J.I. Zink, Q. Xiao, M. Cai, G. Wang, Y. Lu, B. Dunn, Adv. Mater. 30 (2018) e1707476.
[85] B.M. Connolly, M. Aragones-Anglada, J. Gandara-Loe, N.A. Danaf, D.C. Lamb, J. P. Mehta, D. Vulpe, S. Wuttke, J. Silvestre-Albero, P.Z. Moghadam, A.E.H. Wheatley, D. Fairen-Jimenez, Nat. Commun. 10 (2019) 2345.
[86] T. Tian, Z. Zeng, D. Vulpe, M.E. Casco, G. Divitini, P.A. Midgley, J. Silvestre-Albero, J.C. Tan, P.Z. Moghadam, D. Fairen-Jimenez, Nat. Mater. 17 (2018) 174–179.
[87] M.K. Sarango-Ramirez, J. Park, J. Kim, Y. Yoshida, D.W. Lim, H. Kitagawa, Angew. Chem. Int. Ed. 60 (2021) 20173–20177.
[88] O.M. Yaghi, Nat. Mater. 6 (2007) 92–93.
[89] E.M. Miner, S.S. Park, M. Dinca, J. Am. Chem. Soc. 141 (2019) 4422–4427.
[90] J. Cepeda, S. Pérez-Yáñez, G. Beobide, O. Castillo, E. Goikolea, F. Aguesse, L. Garrido, A. Luque, P.A. Wright, Chem. Mater. 28 (2016) 2519–2528.
[91] Y. Peng, V. Krungleviciute, I. Eryazici, J.T. Hupp, O.K. Farha, T. Yildirim, J. Am. Chem. Soc. 135 (2013) 11887–11894.
[92] B. Wu, S. Wang, J. Lochala, D. Desrochers, B. Liu, W. Zhang, J. Yang, J. Xiao, Energ. Environ. Sci. 11 (2018) 1803–1810.
[93] J. Luo, Y. Li, H. Zhang, A. Wang, W.-S. Lo, Q. Dong, N. Wong, C. Povinelli, Y. Shao, S. Chereddy, S. Wunder, U. Mohanty, C.-K. Tsung, D. Wang, Angew. Chem. Int. Ed. 58 (2019) 15313–15317.
[94] C.-C. Su, M. He, R. Amine, T. Rojas, L. Cheng, A.T. Ngo, K. Amine, Energ. Environ. Sci. 12 (2019) 1249–1254.
[95] Q. Tu, L. Barroso-Luque, T. Shi, G. Ceder, Cell Rep. Phys. Sci. 1 (2020).
[96] K. Xu, J. Power Sources 559 (2023).
[97] Y.S. Meng, V. Srinivasan, K. Xu, Science 378 (2022) eabq3750.
[98] Y. Chen, S. Li, X. Pei, J. Zhou, X. Feng, S. Zhang, Y. Cheng, H. Li, R. Han, B. Wang, Angew. Chem. Int. Ed. 55 (2016) 3419–3423.
[99] G.J.H. Lim, Y. Wu, B.B. Shah, J.J. Koh, C.K. Liu, D. Zhao, A.K. Cheetham, J. Wang, J. Ding, ACS Mater. Lett. 1 (2019) 147–153.
[100] P.W. Jaschin, Y. Gao, Y. Li, S.-H. Bo, J. Mater. Chem. A 8 (2020) 2875–2897.
[101] S. Ma, L. Shen, Q. Liu, W. Shi, C. Zhang, F. Liu, J.A. Baucom, D. Zhang, H. Yue, H. B. Wu, Y. Lu, ACS Appl. Mater. Interfaces 12 (2020) 43824–43832.
[102] A.S. Rosen, M.R. Mian, T. Islamoglu, H. Chen, O.K. Farha, J.M. Notestein, R.Q. Snurr, J. Am. Chem. Soc. 142 (2020) 4317–4328.
[103] A.S. Rosen, S.M. Iyer, D. Ray, Z. Yao, A. Aspuru-Guzik, L. Gagliardi, J.M. Notestein, R.Q. Snurr, Matter 4 (2021) 1578–1597.